Biomedicine & Pharmacotherapy 141 (2021) 111857

Contents lists available at ScienceDirect

Biomedicine & Pharmacotherapy

journal homepage: www.elsevier.com/locate/biopha

Synthesis and biological activity of novel 4-aminoquinoline/1,2,3-triazole hybrids against *Leishmania amazonensis*

Nícolas Glanzmann [a,1], Luciana Maria Ribeiro Antinarelli [b,c,1], Isabelle Karine da Costa Nunes [d], Henrique Marcelo Gualberto Pereira [d], Eduardo Antonio Ferraz Coelho [c,e], Elaine Soares Coimbra [b], Adilson David da Silva [a,*]

[a] *Departamento de Química, Instituto de Ciências Exatas, Universidade Federal de Juiz de Fora, Campus Universitário, Juiz de Fora, Minas Gerais 36.036-900, Brazil*
[b] *Departamento de Parasitologia, Microbiologia e Imunologia, Instituto de Ciências Biológicas, Universidade Federal de Juiz de Fora, Campus Universitário, Juiz de Fora, Minas Gerais 36.036-900, Brazil*
[c] *Programa de Pós-Graduação em Ciências da Saúde: Infectologia e Medicina Tropical, Faculdade de Medicina, Universidade Federal de Minas Gerais, Belo Horizonte, Minas Gerais 30.130-100, Brazil*
[d] *Laboratório de Apoio ao Desenvolvimento Tecnológico, Polo de Química, Universidade Federal do Rio de Janeiro, Cidade Universitária Ilha do Fundão, Rio de Janeiro 21.941-598, Brazil*
[e] *Departamento de Patologia Clínica, COLTEC, Universidade Federal de Minas Gerais, Belo Horizonte, Minas Gerais 31270-901, Brazil*

ARTICLE INFO

Keywords:
Leishmania
Antileishmanial activity
Quinoline
1,2,3-triazolic derivative
Apoptosis
Necrosis

ABSTRACT

Quinoline and 1,2,3-triazoles are well-known nitrogen-based heterocycles presenting diverse pharmacological properties, although their antileishmanial activity is still poorly exploited. As an effort to contribute with studies involving these interesting chemical groups, in the present study, a series of compounds derived from 4-aminoquinoline and 1,2,3-triazole were synthetized and biological studies using *L. amazonensis* species were performed. The results pointed that the **derivative 4**, a hybrid of 4-aminoquinoline/1,2,3-triazole exhibited the best antileishmanial action, with inhibitory concentration (IC_{50}) values of ~1 μM against intramacrophage amastigotes of *L. amazonensis* , and being 16-fold more active to parasites than to the host cell. The mechanism of action of **derivative 4** suggest a multi-target action on *Leishmania* parasites, since the treatment of *L. amazonensis* promastigotes caused mitochondrial membrane depolarization, accumulation of ROS products, plasma membrane permeabilization, increase in neutral lipids, exposure of phosphatidylserine to the cell surface, changes in the cell cycle and DNA fragmentation. The results suggest that the antileishmanial effect of this compound is primarily altering critical biochemical processes for the correct functioning of organelles and macromolecules of parasites, with consequent cell death by processes related to apoptosis-*like* and necrosis. No up-regulation of reactive oxygen and nitrogen intermediates was promoted by **derivative 4** on *L. amazonensis* -infected macrophages, suggesting a mechanism of action independent from the activation of the host cell. In conclusion, data suggest that **derivative 4** presents selective antileishmanial effect, which is associated with multi-target action, and can be considered for future studies for the treatment against disease.

1. Introduction

Leishmaniasis is the neglected tropical disease of the highest impact on public health worldwide, with an estimated 30,000 deaths annually. This complex disease is caused by distinct species of protozoa of the genus *Leishmania*, which cause tegumentary or visceral manifestations, depending on mainly the infecting *Leishmania* species and the immune and nutritional status of the mammalian hosts [1,2]. Tegumentary leishmaniasis (TL) can be subclinical or cause self-healing cutaneous lesions which can lead to disfiguring scars accompanied by extensive tissue destruction in nasopharyngeal mucosal tissues. Visceral leishmaniasis (VL) affects organs of the reticuloendothelial system, in particular the spleen, the liver, and the bone marrow, manifesting in the symptomatic form with prolonged fever, hepatosplenomegaly, anemia, and complications related to hemorrhages and concurrent infections [3,4].

* Corresponding author.
E-mail address: david.silva@ufjf.edu.br (A.D. da Silva).
[1] These authors contributed equally to this work.

https://doi.org/10.1016/j.biopha.2021.111857
Received 6 April 2021; Received in revised form 18 June 2021; Accepted 24 June 2021
Available online 13 July 2021

Despite some differences among epidemic countries, the standard treatment against leishmaniasis is based on the use of pentavalent antimonials; and second-line drugs, such as free or liposomal amphotericin B, pentamidine, miltefosine and paramomycin are used as therapeutic options. However, the current treatment has serious drawbacks that limit its efficacy, such as toxicity, high cost and/or emergence of parasite resistance [5,6]. Thus, there is a significant effort to identify more effective and less toxic antileishmanial agents and, in this aspect, a valuable source of new pharmacological agents in medicinal chemistry are based on the quinoline and azole scaffolds, both containing nitrogen-based heterocycles [7–9].

Quinoline derivatives have been exploited as promising bioactive compounds to contribute with novel therapies as antibacterial, anti-HIV, anti-inflammatory, anticancer and antiplasmodial agents [10–13]. 1,2,3-triazole based compounds have been reported for their wide range pharmacological action, presenting application such as anticancer, antimicrobial, anti-tubercular, antiviral, antidiabetic, antimalarial and/or neuroprotective therapy [14–17]. Nowadays, these two privileged groups of bioactive chemical compounds have been investigated as lead compounds in the design of great structural diversity of novel antileishmanial agents [18–22]. In recent works, our research group has conducted several studies evaluating the antileishmanial effect of distinct groups of triazole and quinoline-derivative molecules, in particular of 4-aminoquinolines and 1,2,3-triazoles, some of which showed promising results [18,23–25].

In addition to the pronounced biological activity, 1,2,3-triazoles are also well-known as good connecting groups in organic synthesis. This feature is favored due to the benign reaction conditions, associated with the click chemistry concept, that allows to easily modify the groups in different positions of the 1,2,3-triazolic ring [26]. For this reason, this heterocycle has recently been extensively applied in combination with other functionalities such as eugenol [20], cinnamic acid [27], phenol [28] and naphthoquinone [29] to produce promising antileishmanials. Moreover, it has been reported that combining quinoline and 1,2,3-triazole produced derivatives with activity against *L. donovani* both in the *in vitro* and *in vivo* models [19]. Previously, our research group has used this strategy in a study where new quinoline derivatives, with improved antileishmanial activity, were obtained using 1,2,3-triazoles as connecting groups to introduce steroids in the molecule [26].

In this study, considering the antileishmanial potential of quinoline derivatives, as well as 1,2,3-triazole containing compounds, we synthesized and evaluated the antileishmanial action of compounds derived from 4-aminoquinoline and 1,2,3-triazole and explored the strategy of designing hybrid compounds containing two pharmacophore groups to improve the biological action. In addition, investigations of the main cellular targets, such as mitochondria, plasma membrane, nucleus and others, which are essential for evaluating the mechanism involved in the death of parasites after treatment, were also performed using flow cytometry and spectrofluorimetric analysis.

2. Material and methods

2.1. Synthesis of the tested compounds

All of the tested compounds, and their relationship to each other in the synthetic route, can be found in Scheme 1. The chemicals used in this work were supplied by Sigma-Aldrich. The melting ranges of the synthesized compounds were acquired using a MQAPF-301-Microchemical digital apparatus. A BRUKER AVANCE III 500 MHz spectrometer was used to obtain ^{1}H, ^{13}C and 2D Nuclear Magnetic Resonance spectra. Chemical shifts (δ) are expressed as ppm in relation to TMS. A Q-Exactive Plus Orbitrap high resolution mass spectrometer (ThermoFisher Scientific, Bremen, Germany) was used to perform HRMS analysis, using the electrospray ionization method (ESI) operating in positive and negative mode through direct injection analysis.

2.1.1. Synthesis of the quinolines *1* and *2*

The compounds were synthesized according to the previously published procedures [26,30].

2.1.2. Synthesis of the quinoline/1,2,3-triazole hybrid *4*

To a round-bottom flask, 0.90 mmol **derivative 2** and 1.25 mmol 1-

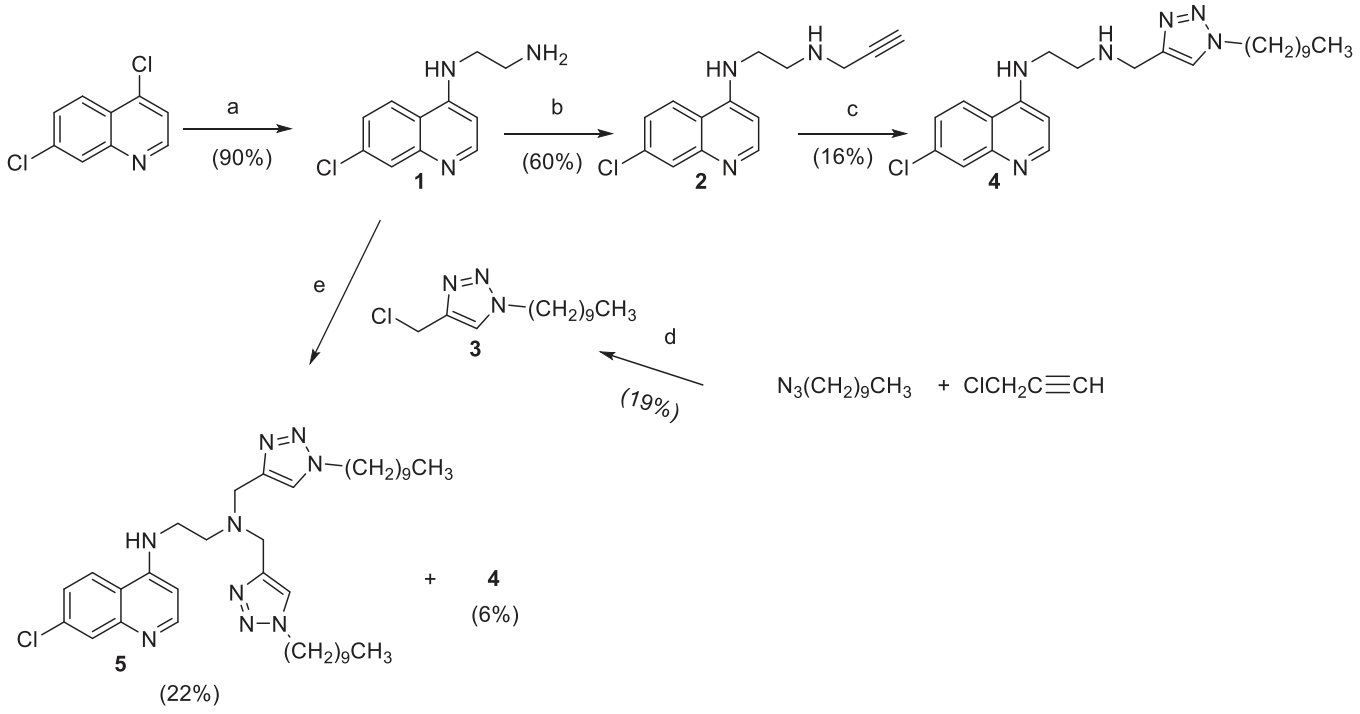

Scheme 1. Synthetic route for the tested compounds.[a]ethane-1,2-diamine, 80 °C. [b]propargyl bromide, K_2CO_3, ethanol, 0–25 °C. [c]1-azidodecane, Copper (II) sulfate hydrate, sodium ascorbate, room temperature. [d]Copper (II) sulfate hydrate, sodium ascorbate, room temperature. [e] **derivative 3**, ethanol, 60 °C.

azidodecane, previously synthesized according to Ren et al. (2011) [31], were dissolved in 15 mL of an ethanol and water mixture (4:1). In sequence, 0.044 mmol Copper (II) sulfate pentahydrate and 0.36 mmol sodium ascorbate were slowly added under stirring. The reactant mixture was kept at room temperature for 7 days and, after that, water was added and the mixture was extracted with CH_2Cl_2. The organics were dried (anhydrous sodium sulfate), the CH_2Cl_2 was evaporated under reduced pressure and thin layer chromatography (TLC) analysis, using the eluent CH_2Cl_2/CH_3OH (9:1), determined the presence of the product (Retention factor = 0.4). The desired product was isolated from the starting material residues through column chromatography (CH_2Cl_2/CH_3OH gradient). After removing the solvent from the pure fractions, **derivative 4** was obtained with a 15.5% yield as a light yellow solid. Melting range = 90–93 ºC. ^{1}H NMR (500 MHz, $CDCl_3$) δ (ppm), *J* (Hz): 0.87 (t, *J* = 6.9, 3H); 1.15 – 1.37 (m, 14H); 1.87 (quint, *J* = 7.6, 2H); 2.05 (bs, 2H, NH_2); 3.10 (t, *J* = 5.6, 2H); 3.38 (t, *J* = 5.7, 2H); 3.99 (s, 2H); 4.31 (t, *J* = 7.3, 2H); 6.25 (bs, 1H, NH); 6.36 (d, *J* = 5.5, 1H); 7.38 (dd, *J* = 8.9 e 2.2, 1H); 7.42 (s, 1H); 7.89 (d, *J* = 8.9, 1H); 7.95 (d, *J* = 2.2, 1H); 8.49 (d, *J* = 5.4, 1H). ^{13}C NMR (126 MHz, $CDCl_3$) δ (ppm): 14.2; 22.8; 26.6; 29.1; 29.4; 29.5; 29.6; 30.4; 32.0; 42.5; 44.0; 46.9; 50.5; 99.1; 117.5; 121.4; 122.0; 125.5; 128.3; 135.2; 146.2; 148.7; 150.4; 151.6. HR-ESI-MS: *m/z* calculated for $C_{24}H_{36}ClN_6$ $[M+H]^+$ 443.26845, found 443.26837.

2.1.3. Synthesis of the intermediate 1,2,3-triazole *3*

The same conditions as the previous procedure were used, substituting the alkyne to propargyl chloride. Thin layer chromatography (TLC) analysis, using the eluent CH_2Cl_2/CH_3OH (95:5), determined the presence of the product (Retention factor = 0.8). **Derivative 3** was obtained with an 18.7% yield as a white solid. Melting range = 39–41 ºC. ^{1}H NMR (500 MHz, $CDCl_3$) δ (ppm), *J* (Hz): 0.86 (t, *J* = 6.9, 3H); 1.11 – 1.54 (m, 14H); 1.89 (quint, *J* = 7.2, 2H); 4.33 (t, *J* = 7.3, 2H); 4.70 (s, 2H); 7.57 (s, 1H). ^{13}C NMR (126 MHz, $CDCl_3$) δ (ppm): 14.2; 22.8; 26.6; 29.1; 29.3; 29.5; 29.6; 30.4; 32.0; 36.4; 50.7; 122.6; 144.8. HR-ESI-MS: *m/z* calculated for $C_{13}H_{25}ClN_3$ $[M+H]^+$ 258.17315, found 258.17307.

2.1.4. Synthesis of the quinoline/1,2,3-triazole hybrid *5*

To a round-bottom flask, 0,58 mmol of **derivative 3** and 0,86 mmol of **derivative 1** were added and dissolved in 5 mL of ethanol. The reactant mixture was submitted to constant stirring at 60 ºC for 3 days, when thin layer chromatography (TLC) analysis, using the eluent CH_2Cl_2/CH_3OH (9:1), showed two products, identified as **derivative 5** (Retention factor = 0.6) and **derivative 4**. At this point, the reaction was stopped, the ethanol was removed under reduced pressure and the products were isolated through column chromatography (CH_2Cl_2/CH_3OH gradient). After removing the solvent from the pure fractions, the previously described **derivative 4** was obtained with a 5.6% yield and the reaction also yielded the major product **derivative 5** (21.6%) as a light brown solid. Melting range = 79–81 ºC. ^{1}H NMR (500 MHz, $CDCl_3$) δ (ppm), *J* (Hz): 0.87 (t, *J* = 7.0, 6H); 1.20 – 1.32 (m, 28H); 1.83 (quint, *J* = 7.0, 4H); 1.96 (bs, 2H, NH); 2.96 (t, *J* = 5.4, 2H); 3.36 (q, *J* = 4.7, 2H); 3.88 (s, 4H); 4.28 (t, *J* = 7.3, 4H); 6.30 (d, *J* = 5.4, 1H); 6.87 (bs, 1H, NH); 7.45 (dd, *J* = 8.9 e 2.2, 1H); 7.51 (s, 2H); 7.94 (d, *J* = 2.1, 1H); 8.25 (d, *J* = 9.0, 1H); 8.48 (d, *J* = 5.3, 1H). ^{13}C NMR (126 MHz, $CDCl_3$) δ (ppm): 14.2; 22.8; 26.6; 29.1; 29.4; 29.5; 29.6; 30.4; 32.0; 41.0; 48.3; 50.5; 50.8; 98.9; 117.8; 122.7; 122.9; 125.4; 128.4; 135.0; 144.4; 149.1; 150.5; 152.0. HR-ESI-MS: *m/z* calculated for $C_{37}H_{59}ClN_9$ $[M+H]^+$ 664.45765, found 664.45789.

2.1.5. Further NMR characterization of *derivative 4*

The main compound used for the mechanism of action assays in this work was fully characterized via unidimensional and bidimensional NMR techniques which can be found in the supplementary material. The ^{1}H and ^{13}C NMR described above were fully attributed based on *COSY*, *HSQC* and *HMBC* correlation spectroscopy. Although the presence of the 1,2,3-triazolic signals in the ^{1}H (δ 7.42 ppm) and ^{13}C NMR spectra (δ 121.4 and 146.2 ppm) is the main evidence of product formation, it is also important to note that the *NOESY* correlation spectra (Fig. 1) can endorse the connectivity between the 1,2,3-triazole nucleus and the remaining molecular moieties. For the main synthetic route used to obtain the **derivative 4**, the correlation peaks between the 1,2,3-triazolic hydrogen (H-7′) and the hydrogens H-5′ and H-9′, highlighted in Fig. 1, provides solid proof that the 1,2,3-triazolic ring is connected both to the alkyl side chain and the quinoline containing remnant of the molecule. Nonetheless, in the specific case of the **derivative 4** obtained as a side product in the synthesis of **derivative 5**, the correlation peak between hydrogens H-5′ and H-3′ confirms the connection between the 1,2,3-triazolic and quinolinic parts of the hybrid.

2.2. Ethics, animals and parasites

Female BALB/c mice (4–6 weeks old) were purchased from the Institute of Reproduction Biology of UFJF and maintained under controlled conditions: temperature at 22 °C, cycle of 12/12 h light/dark, water and food ad libitum. The study was approved by the Committee for the Ethical Handling of Research Animals (protocol number 007/2018 and 008/2018) from Federal University of Juiz de Fora (UFJF, Juiz de Fora, Minas Gerais, Brazil). *Leishmania amazonensis* (IFLA/BR/1967/PH8) strain was cultivated at 25 °C in Warren's medium [brain heart infusion (BHI) containing hemin and folic acid] at pH 7.2, supplemented with 10% Fetal Bovine Serum (FBS), and 0.1% of the antibiotic solution composed by 100 UI/mL penicillin G and 0.1 mg/mL of streptomycin [24].

2.3. In vitro antipromastigote activity

Leishmania amazonensis promastigotes (2×10^6), which were collected in an exponential growth phase, were incubated in the presence of **derivatives 1–5** (1.6–100.0 μM) in 96-well culture plates (Nunc, Nunclon, Roskilde, Denmark) for 72 h at 25 °C. Miltefosine at 3.1–100.0 μM (Cayman Chemical Company, Michigan, USA) was used as drug control. The parasite viability was assessed by measuring of the MTT (3-(4.5-dimethylthiazol-2-yl)-2.5-diphenyl tetrazolium bromide, Sigma-Aldrich, USA) colorimetric method. The optical density (OD) values were read in a microplate spectrophotometer reader (Multiskan MS microplate reader, LabSystems Oy, Helsink, Finland) at 570 nm [32]. The results were expressed as the inhibitory concentration of 50% of parasite growth (IC_{50}) and were calculated from three independent experiments performed in duplicate.

2.4. Treatment of Leishmania-infected macrophages

Murine macrophages (6×10^5 cells) were platted in 24-well plates containing sterile glass coverslips in RPMI 1640 medium supplemented with 10% FBS, and incubated for 24 h at 37 °C in 5% CO_2. After that, cultures were infected with stationary promastigotes of *L. amazonensis* (6×10^6 cells, at a ratio of 10 parasites per one macrophage) for 4 h, at 33 °C in 5% CO_2. In sequence, free parasites were removed by extensive washing with PBS 1x, and infected macrophages were treated with increasing concentrations (0.2–100.0 μM) of **derivatives 1–5**, for 72 h at 33 °C in 5% CO_2. Miltefosine (0.8–25.0 μM) was used as control drug in this assay. After incubation, cells were fixed with absolute ethanol and stained with Giemsa, A total of 200 non-parasited or parasited macrophages were counted in a light microscope [32]. The results were calculated as a percentage of reduction of the global burden of the amastigotes per infected cell in relation to the non-treated control. From these results, the IC_{50} of each molecule was determined using the Probit program.

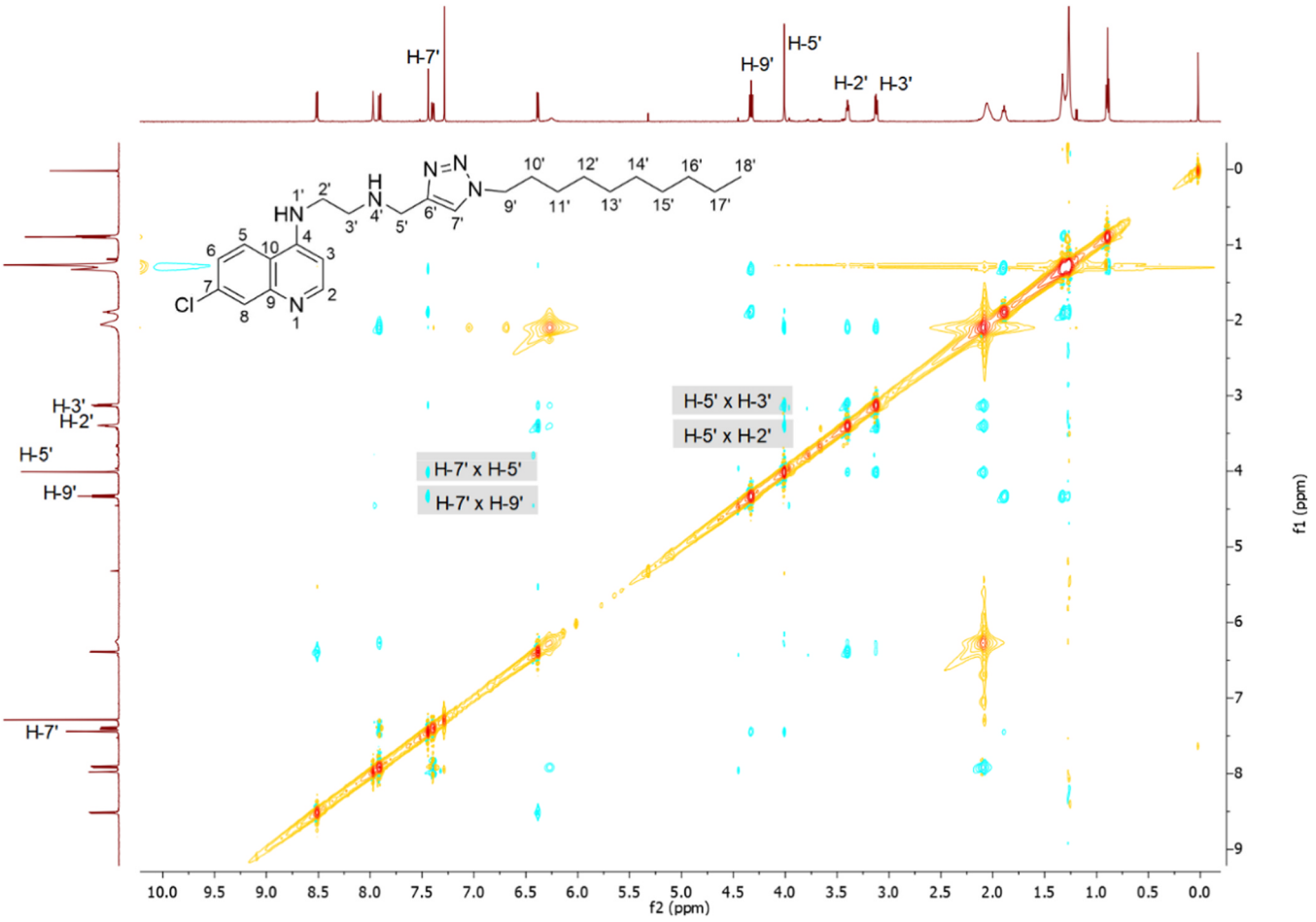

Fig. 1. *NOESY* correlation spectra of **derivative 4**.

2.5. Cytotoxicity assay in murine macrophages

To evaluate the cytotoxicity in murine macrophages, cells were collected from the peritoneal cavity of BALB/c mice and plated (2×10^5 per well) in RPMI-1640 medium supplemented with 10% FBS in a 96-well culture plate, and maintained at 37 ºC in 5% CO_2. After 24 h, cells were treated with different concentrations of **derivatives 1–5** (9.4–150.0 μM) or miltefosine (9.4–150.0 μg/mL) for 72 h at 37 °C. The cell viability was also evaluated by the MTT method. The cytotoxic concentration that decreases viability of macrophages by 50% (CC_{50}) was calculated from three independent experiments performed in duplicate [32]. Selectivity index (SI) values were calculated by the ratio between the results of CC_{50} for macrophages and IC_{50} for parasites for each substance.

2.6. Mechanism of antileishmanial action of ***derivative 4***

All studies were done with the best antileishmanial compound (**derivative 4)**, and the concentrations used corresponded to values close to 1 or 2 times IC_{50} of promastigote forms (5.0 and 10 μM, respectively) or amastigotes (1.2 and 2.4 μM, respectively) of *L. amazonensis* obtained after 72 h of treatment.

2.6.1. Determination of mitochondrial membrane potential (Δψm)

Leishmania amazonensis promastigotes (1×10^7 cells per mL) in the exponential phase were incubated with **derivative 4** (5.0 or 10 μM) for 24 h, at 25 °C. Afterward, the parasites (5×10^6 cells/mL) were incubated with 5 μg/mL JC-1 (Sigma-Aldrich, St. Louis, MO, USA) for 30 min in the dark at 37 °C. After washing twice with Hanks′ Balanced Salt solution (HBSS), fluorescence was measured by using a FACsCanto II flow cytometer (Becton Dickinson, Rutherford, NJ, USA) equipped with DIVA software (Joseph Trotter, Scripps Research Institute, La Jolla, CA, USA), and a total of 10,000 events were analyzed per sample.

Measurement of ΔΨm was also carried out using the Mitotracker Red (Invitrogen, Eugene, OR, USA) fluorescent probe. In brief, promastigotes (10×10^6 cells/mL) were stained with Mitotracker at 500 nM in the dark for 40 min at 37 °C. After washing twice with PBS 1x, samples were added to a black 96-well plate and fluorescence was measured in a fluorometer (FLx800, BioTek Instruments, Inc., Winooski, VT, USA) at 540/600 nm excitation/emission. As control, promastigotes were incubated with carbonyl cyanide *p*-trifluoromethoxyphenylhydrazone (FCCP; Sigma-Aldrich, USA) at 5.0 μM for 10 min [24,33].

2.6.2. Evaluation of mitochondrial stress

For this assay, H_2DCFDA and MitoSOX were used. H_2DCFDA is a probe that estimates several intracellular reactive oxygen species (ROS) levels. Although in this case the major detected ROS consists of H_2O_2, other species such as hydroxyl radical, hydroperoxides, and peroxynitrite can also be detected [34]. The MitoSOX is a fluorescent probe highly selective to mitochondria used as a sensor for detecting mitochondrial superoxide [25,35]. In brief, *L. amazonensis* promastigotes (1×10^7 cells per mL) in the exponential phase were non-treated or treated with **derivative 4** (5.0 or 10 μM) for 24 h at 25 °C. Afterward, promastigotes were washed with PBS, and a parasite suspension (2×10^7 cells per well) was incubated with 2′,7′-dichlorodihydrofluorescein diacetate (H_2DCFDA; Invitrogen, Eugene, OR, USA) at 20 μM or MitoSOX Red indicator (Invitrogen, Eugene, OR, USA) at 5 μM for 30 min in the dark at room temperature. The fluorescence values were

measured at 485/528 nm and 540/600 nm excitation/emission for H_2DCFDA and MitoSOX, respectively, by using a fluorimetric microplate reader (FLx800, BioTek Instruments, USA). As positive controls for H_2DCFDA and MitoSOX assays, promastigotes were incubated with miltefosine at 22.0 μM or antimycin A at 10.00 μM, respectively [25].

2.6.3. Detection of lipid neutral accumulation

Leishmania amazonensis promastigotes (1×10^7 cells per mL) were treated with **derivative 4** (5.0 or 10 μM) for 24 h at 25 °C. Parasites were harvested in PBS, and concentration was adjusted to 5×10^6 cells in 200 μL of PBS 1x. Then, the suspension was incubated with 10 μg/mL Nile Red (Sigma-Aldrich, St. Louis, MO, USA) for 20 min. Afterward, the fluorescence intensity was measured fluorimetrically (FLx800, BioTek Instruments, Inc., Winooski, VT, USA), by using 485 and 528 nm as excitation and emission wavelengths, respectively [36].

2.6.4. Determination of phosphatidylserine exposure on the plasma membrane

Leishmania amazonensis promastigotes (1×10^7 cells per mL) were treated with **derivative 4** (5.0 or 10 μM) or miltefosine (44.0 μM) for 24 h at 25 °C. After washing with PBS, parasites were incubated with annexin V-FITC (Invitrogen, Eugene, OR, USA) and propidium iodide (PI 1.0 μg/mL, Sigma-Aldrich, St. Louis, MO, USA), for 20 min in the dark. Afterward, samples were analyzed using a FACsCanto II flow cytometer (10,000 events) (Becton Dickinson, Rutherford, NJ, USA), by using the FITC parameters (Annexin V-FITC) and PE (for PI) [36].

2.6.5. Analysis of cell cycle

Leishmania amazonensis promastigotes (1×10^7 cells per mL) were treated with **derivative 4** (5.0 or 10 μM) for 24 h at 25 ºC. Then, parasites were permeabilized with 70% ethanol for 1 h at 4 °C, followed by the addition of 200 μg/mL of Ribonuclease A (Sigma-Aldrich, St. Louis, MO, USA) for 1 h at 37 °C. Cells were stained with PI solution (1.0 μg/mL; Sigma-Aldrich, St. Louis, MO, USA) for 20 min in the dark, after which samples were analyzed in a FACsCanto II flow cytometer (Becton Dickinson, Rutherford, NJ, USA) equipped with DIVA software (Joseph Trotter, Scripps Research Institute, La Jolla, CA, USA) [36].

2.6.6. DNA fragmentation assay

DNA fragmentation was determined by the enzyme terminal deoxynucleotidyl transferase dUTP nick end labeling (TUNEL) assay using In Situ Cell Death Detection Kit (Roche, IN, USA), according to the manufacturer's instructions. After 24 h of treatment with **derivative 4** (5.0 or 10 μM), promastigotes were washed with PBS and fixed in solution of 2% paraformaldehyde for 15 min. Parasites were, then, washed twice with PBS, permeabilized with a solution of 0.2% Triton x-100 and then labeled with the TUNEL solution for 1 h at 37ºC. Afterward, cells were resuspended in PBS, added to a black 96-well plate and the fluorescence intensity was measured in a fluorimetric microplate reader (FLx800, BioTek Instruments, USA) at 485/528 nm of excitation/emission [18]. Promastigotes incubated with DNase (New England Biolabs, MA, USA) at 5 μg/mL for 10 min were used as a positive control.

2.6.7. Evaluation of the cell membrane integrity

Leishmania amazonensis promastigotes (1×10^7 cells per mL) were treated with **derivative 4** (5.0 or 10.0 μM) for 24 h at 25 ºC. Parasites were washed with PBS and stained with PI (Sigma-Aldrich, St. Louis, MO, USA) at 1.0 μg/mL, in the dark for 15 min. PI-stained parasites were analyzed using a FACsCanto II flow cytometer (Becton Dickinson, Rutherford, NJ, USA) and PE channels, acquiring a total of 10,000 events. As positive control for this assay, parasites incubated at 65 ºC for 10 min were used [33].

2.6.8. Measurement of oxidative stress in L. amazonensis-infected macrophages

Macrophages were *L. amazonensis* -infected or non-infected, and they were treated with **derivative 4** (1.2 and 2.4 μM) for 24 h at 33 ºC in 5% CO_2. Then, cells were washed with PBS and incubated with H_2DCFDA (20 μM; Sigma-Aldrich, St. Louis, MO, USA) and DAF-FM diacetate (5 μM; Sigma-Aldrich, St. Louis, MO, USA) for 30 min in the dark at 33 °C in 5% CO_2. Measurements of fluorescence were performed using a fluorimetric microplate reader (FLx800, BioTek Instruments, USA), by using 485 and 528 nm as excitation and emission wavelengths, respectively. Macrophages stimulated with H_2O_2 (4 mM) were used as positive control [37].

2.7. Statistical analysis

The compound concentrations necessary to inhibit 50% of *Leishmania* viability (IC_{50} values) and macrophages (CC_{50} values) were calculated using the Probit program. Results obtained in the mechanism of action were representative of three independent experiments, performed in triplicate. The one-way analysis of variance (ANOVA) accompanied by the Dunnett's test were used for comparisons between the groups. Differences between the groups were considered significant with $P < 0.05$ (*), $P < 0.01$ (**), and $P < 0.001$ (***).

3. Results

The *in vitro* antileishmanial effect of a series of five derivatives of quinoline (**derivatives 1** and **2**), 1,2,3 triazole (**derivative 3)** and quinoline triazole hybrids (**derivatives 4** and **5**) were investigated against promastigote and amastigote forms of *L. amazonensis* (Table 1). From the evaluated compound series, derivatives **2**, **3** and **4** were effective against both parasite stages of the evaluated *Leishmania* species. Among these, **derivative 4** showed the best antileishmanial effect, with IC_{50} values of 5.7 (4.4–7.4) μM and 1.1 (1.0–1.2) μM against promastigotes and amastigotes of *L. amazonensis* , respectively, being better than miltefosine (IC_{50} of 22.0 (21.5–22.5) μM and 4.2 (4.0–4.4) μM, respectively) (Table 1).

The cytotoxic effect of the tested compounds was evaluated against murine peritoneal macrophages (Table 1). The derivatives **3**, **4** and **5** demonstrated moderate cytotoxicity, with CC_{50} values of 21.2 (17.8–25.2) μM, 18.2 (14.9–22.2) μM and 38.8 (32.0–47.1) μM, respectively. Based in the results, the selectivity index (SI) was calculated (Table 1), and the best antileishmanial compound (**derivative 4**) was at minimum 16 times more potent against the amastigote forms of *L. amazonensis* than to the host cell.

Considering that **derivative 4** showed higher antileishmanial activity, the mechanism of action in *Leishmania* spp was investigated. As a well-known model, the *L. amazonensis* species was used in these studies. The mitochondrial dysfunction in *L. amazonensis* promastigotes treated with **derivative 4** was assessed by analysis of the depolarization of mitochondrial membrane potential (ΔΨm) and induction of oxidative stress.

Analysis of the mitochondrial membrane potential (ΔΨm) by flow cytometry using JC-1 fluorescent marker demonstrated that **derivative 4** caused a decrease on ΔΨm sustained by a fluorescence shift from red to green with an increase in the population of parasites with green fluorescence (lower quadrant) corresponding to 5.2% and 46.2% of parasites after treatment with 5 and 10 μM of **derivative 4**, respectively, compared to non-treated control (2.2%). FCCP, a known inhibitor of the respiratory chain, at 5 μM showed an increase of 87.7% in green fluorescence of parasites (Fig. 2a). Moreover, the relative ΔΨm value was quantified using the ratio of red and green fluorescence. As shown in Fig. 2b, the JC-1 ratio was 42.09 in non-treated control, while its value decreased to 18.1 and 1.21 in the groups treated with 5 and 10 μM of **derivative 4**, respectively. In FCCP-treated parasites the ratio was 0.16.

The fluorimetric results using the Mitotracker dye also showed that the **derivative 4** caused a significant ΔΨm reduction of 23.9% and 37.6% after treatment with 5 and 10 μM, respectively (Fig. 2**c**). A similar effect was found in promastigotes incubated with FCCP (5 μM) with

Table 1
In vitro antileishmanial activity against *L. amazonensis*, cytotoxicity in murine macrophages and selectivity index of **derivatives 1–5**.

Derivatives	IC_{50}[a] µM (95% C.I.)[c]		CC_{50}[b] µM (95% C.I.)[c]	Selectivity Index (SI)[d]	
	Promastigotes	Amastigotes	Macrophages	Pro	Ama
1	>100	29.9 (25.6–34.8)	>100[e]	–	>3.4
2	78.3 (59.1–103.8)	30.3 (25.8–35.7)	>100[e]	>1.3	>3.3
3	5.5 (4.8–6.4)	12.7 (10.3–15.5)	21.2 (17.8–25.2)	3.8	1.7
4	5.7 (4.4–7.4)	1.1 (1.0–1.2)	18.2 (14.9–22.2)	3.2	16.5
5	>100	>50	38.8 (32.0–47.1)	–	–
Miltefosine	22.0 (21.5–22.5)	4.2 (4.0–4.4)	89.6 (75.7–106.1)	4.1	21.3

[a] IC_{50} = Inhibitory concentration of 50% of parasites.
[b] CC_{50} = Cytotoxic concentration of 50% of murine macrophages.
[c] 95% confidence intervals are in brackets.
[d] Selectivity Index (SI) = CC_{50} in macrophages/IC_{50} in promastigote (Pro) and amastigote (Ama) stages.
[e] Results were previously published [23]. Miltefosine was used as positive control. The data represent the average of three independent experiments.

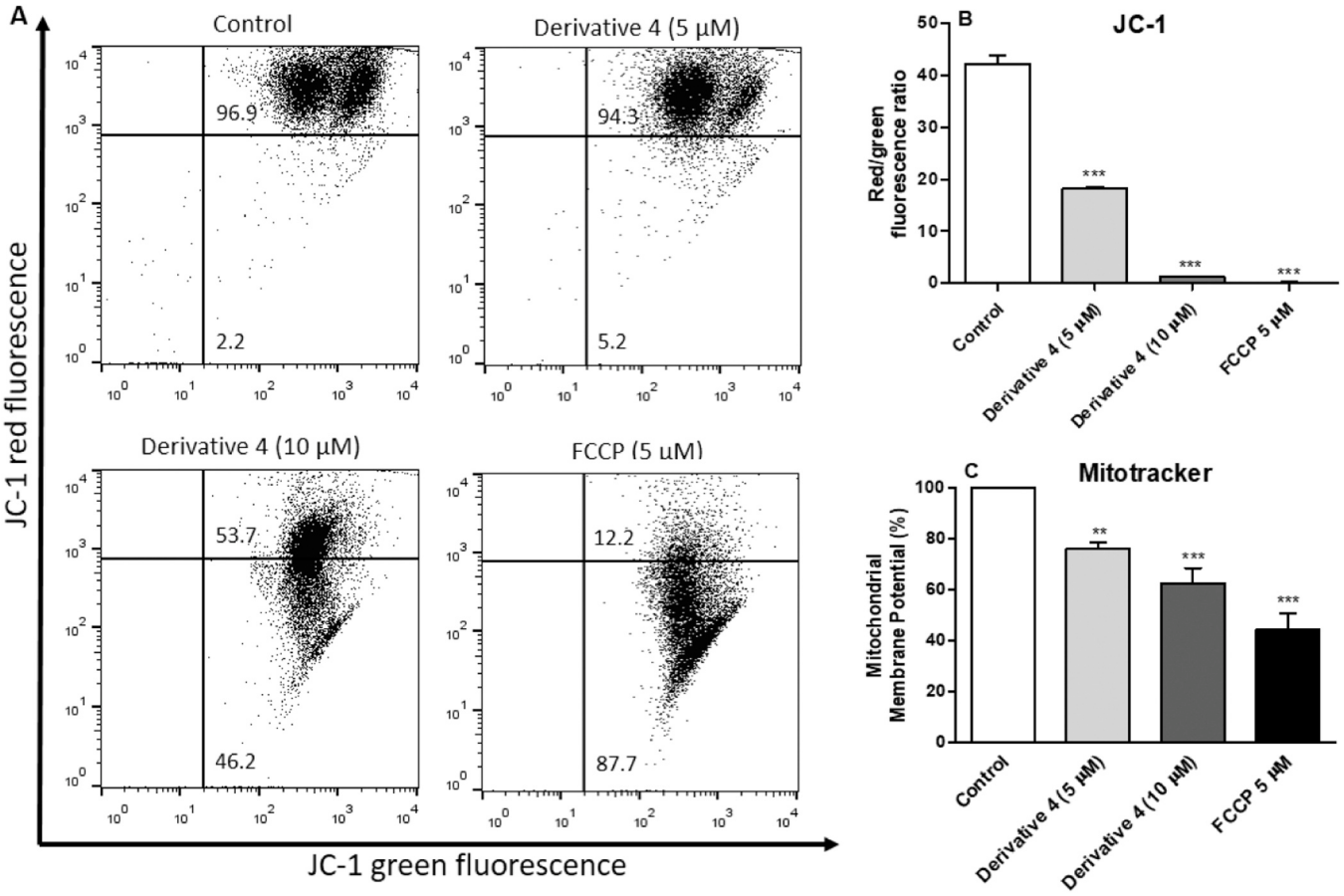

Fig. 2. Evaluation of depolarization of the mitochondrial membrane potential (ΔΨm) in *L. amazonensis* promastigotes after treatment with derivative 4. Promastigotes of *L. amazonensis* were non-treated (negative control) or treated with **derivative 4** (5.0 or 10.0 µM) and, after 24 h, measurement of ΔΨm was performed using the fluorescent markers JC-1 **(A** and **B)** and Mitotracker **(C)**. In the JC-1 assay, data acquisition of fluorescence was performed by flow cytometry using two conventional channels, FL1 (green fluorescence) and FL2 (red fluorescence) **(A).** Relative ΔΨm value was calculated using the ratio between the red to green fluorescence **(B)**. For Mitotracker analysis **(C)**, the fluorescence intensity was measured by fluorimetry and the results were expressed as the percentage of reduction of ΔΨm in relation to the negative control regarded as 100%. FCCP at 5.0 µM was used as positive control for ΔΨm. In both assays, three independent experiments in triplicate were performed. (*), (**) and (***) represents statistically significant difference in relation to the non-treated control ($P < 0.1$, $P < 0.01$ and $P < 0.001$, respectively).

reduction of 55.6% in the ΔΨm.

The mitochondrial oxidative stress in **derivative 4**-treated promastigotes was evaluated by quantification of ROS levels using two fluorescent probes: H_2DCFDA and MitoSOX Red. The treatment of *L. amazonensis* promastigotes with **derivative 4** led to an increase in ROS levels when using the both probes (Fig. 3**a** and **b**). Treated parasites at 5.0 and 10.0 µM induced an increase in ROS levels of 54.7% and 50.4%, respectively, with H_2DCFDA probe (Fig. 3**a**); and of 79.4% and 99.4%, respectively, with MitoSOX Red (Fig. 3**b**). The positive controls, miltefosine (Fig. 3**a**) and antimycin A (Fig. 3**b**), induced an increase in ROS of 98.8% and 152%, respectively.

In addition, higher content of neutral lipids was found in parasites treated with **derivative 4** with an increase of 68.0% and 117.5% after treatment with 5 and 10 µM, respectively, in relation to non-treated control (Fig. 4).

The induction of the phosphatidylserine (PS) exposure in the plasma

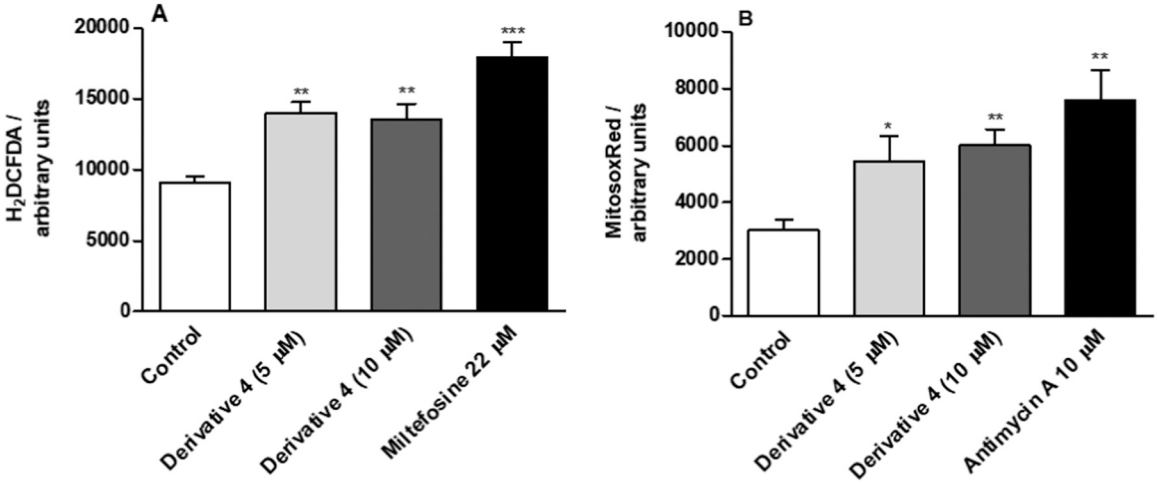

Fig. 3. Mitochondrial oxidative stress in *L. amazonensis* promastigotes treated with derivative 4. Promastigotes of *L. amazonensis* were non-treated (negative control) or treated with **derivative 4** (5.0 or 10.0 μM) and after 24 h were incubated with the fluorescent probes H_2DCFDA **(A)** and MitosoxRed **(B)** for determination of ROS levels. In both assays, the fluorescence intensity was measured by fluorimetry and the results were expressed in arbitrary units consisting of the means of three independent experiments. (*), (**) and (***) represents statistically significant difference in relation to the non-treated control ($P < 0.1$, $P < 0.01$ and $P < 0.001$, respectively).

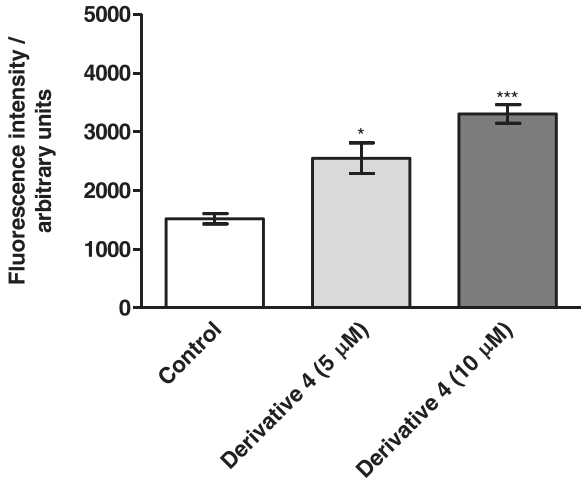

Fig. 4. Accumulation of neutral lipids in *L. amazonensis* promastigotes treated with the derivative 4. Promastigotes (1×10^7 cells) were non-treated (negative control) or treated with **derivative 4** (5.0 and 10.0 μM) for 24 h at 25 °C and marked with Nile Red. (*) and (***) represents statistically significant difference in relation to the non-treated control ($P < 0.1$ and $P < 0.001$, respectively).

membrane surface after treatment with **derivative 4** was assayed using double staining with Annexin V-FITC and PI and the analysis was performed by flow cytometry. **Derivative 4** at 10.0 μM caused an increase in the percentage of promastigotes in early apoptosis-*like* (annexin V^+, PI^-), late apoptosis-*like* (annexin V^+, PI^+) and necrosis (annexin V^-, PI^+) of 17.3%, 31.9% and 22.3%, respectively, when compared to the non-treated control (2%, 11.2% and 0.9%). Miltefosine (44.0 μM) was used as a positive control, and significantly increased the percentage of parasites in early and late apoptosis-like by 16.6% and 21.2%, respectively, compared to the non-treated control (Fig. 5).

By flow cytometry analysis, changes in the cell cycle progression of parasites after treatment with **derivative 4** was investigated (Fig. 6). According to the histogram results, treatment with **derivative 4** at 10 μM induced a significant increase in the percentage of promastigotes in the sub G_0/G_1 phase (41%) when compared to the non-treated parasites (12%), which was accompanied by decreasing in percentage of parasites in the G_0/G_1, S and G_2/M phases (25.1%, 10.8% and 14.0%, respectively), in comparison to control parasites (34.4%, 14.4% and 19.5%, respectively).

The occurrence of DNA fragmentation in promastigotes treated with **derivative 4** was determined by the TUNEL assay. Treatment with **derivative 4** at 10 μM significantly increased DNA fragmentation by 15% compared with the non-treated parasites. Parasites incubated with DNase (positive control) caused increase in DNA fragmentation by 22% (Fig. 7).

The permeabilization of plasma membrane in promastigotes treated with **derivative 4** was assessed using PI. Results showed an increase in the percentage of PI-positive promastigotes after treatment with **derivative 4** at the concentration of 10 μM (44.7%) when compared to the non-treated control (12.2%), indicating damage to the plasma membrane of parasites (Fig. 8).

Considering that **derivative 4** was highly effective in reducing the number of intramacrophage amastigotes of *Leishmania* spp, investigations were conducted to evaluate whether the mechanism of cellular death of intracellular parasites is associated with the activation of microbicidal mechanisms by macrophages. However, **derivative 4** showed no induction of NO and ROS production in both non-infected and infected macrophages (data not shown).

4. Discussion

In the present study, a new series of derivatives of quinoline, 1,2,3-triazole and quinoline triazole hybrids was synthesized and displayed antileishmanial activity against *L. amazonensis*, an important *Leishmania* species in the American countries capable of causing not only diverse cutaneous manifestations but also atypical visceral leishmaniasis [38]. Among the tested compounds, **derivative 4**, a quinoline triazole hybrid was identified as the most promising of this set, exhibiting higher antileishmanial activity (IC_{50} values ≤ 10 μM) and higher selectivity index, being 16-fold more active to intracellular parasites than to mammalian cells. It is interesting to note the synergistic effect in which **derivative 4**, a hybrid of 4-aminoquinoline and 1,2,3-triazole, presented lower IC_{50} values than the non-hybrid precursors **1**, **2** and **3**. This shows that, in this particular case, the presence of both quinolinic and 1,2,3-triazolic rings favored the antileishmanial activity. A similar feature was also observed in other works that combined these two groups through a molecular hybridization approach, providing promising antileishmanial effects or properties [19,26], antiplasmodial [39–42], anticancer [43], antibacterial [44–46] and antifungal agents [45–47], as well as

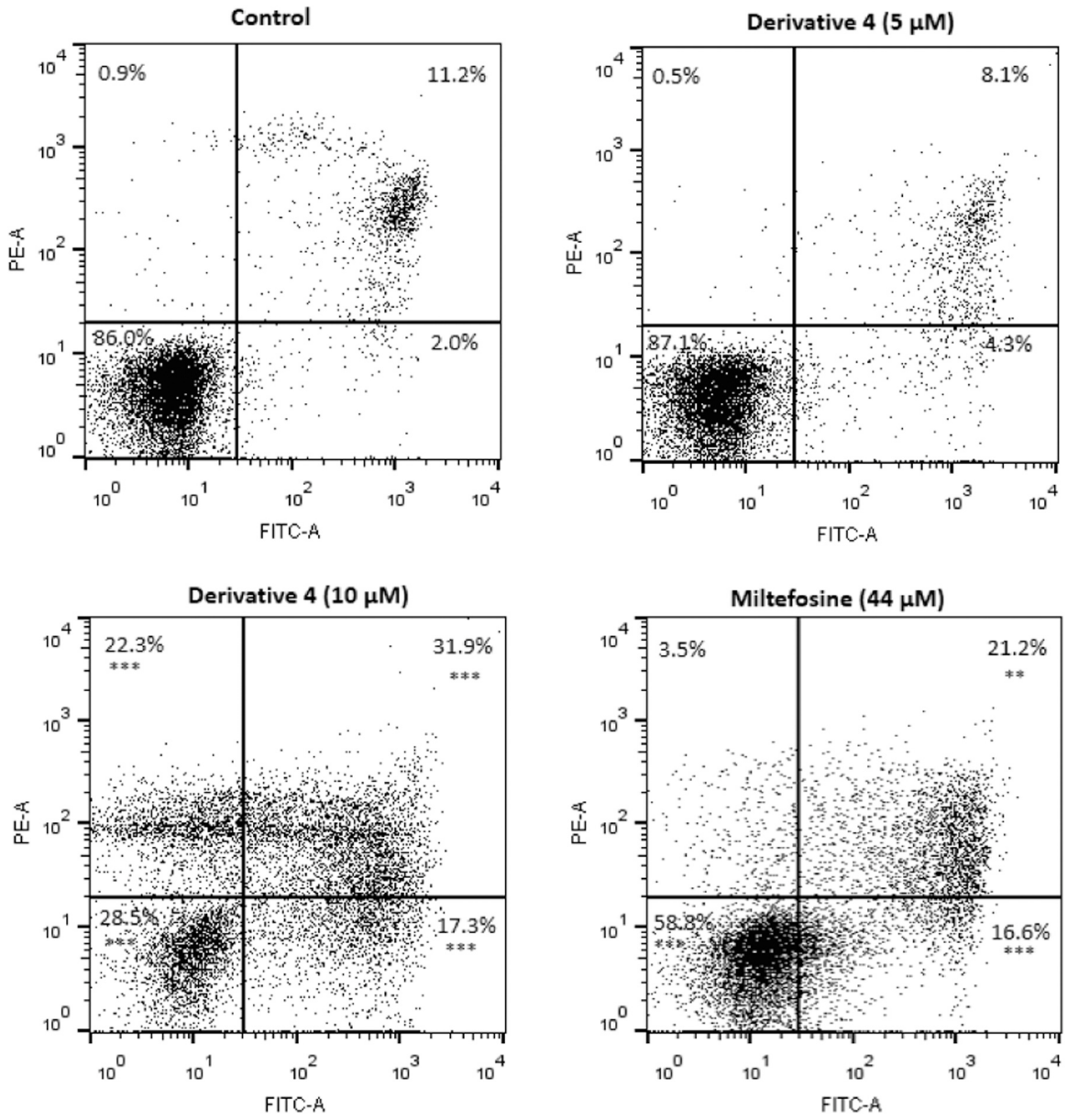

Fig. 5. Determination of phosphatidylserine exposure on the cell membrane in promastigotes of *L. amazonensis* treated with derivative 4**.** Promastigotes (10^7 cells/mL) were treated with **derivative 4** (at 5 or 10 µM) for 24 h. Then, the cells were double stained with the fluorescent probes annexin V-FITC and propidium iodide (PI), and events were acquired by flow cytometry. Representative dot plots of three independent experiments with similar results. (**) and (***) represents statistically significant difference in relation to the non-treated control ($P < 0.01$ and $P < 0.001$, respectively).

acetylcholinesterase inhibitor agents [48], thus reasserting this strategy as a pathway to new bioactive compounds.

In light of the promising *in vitro* results shown by **derivative 4**, investigations were conducted to evaluate the mechanism of cellular death induced by this compound in *Leishmania* spp. For this, mitochondria were chosen as the primary target to be investigated. The mitochondria of trypanosomatids are vital organelles for parasite survival, playing a pivotal role in the regulation of distinct physiologic processes including bioenergetics, ATP generation, control of redox metabolism, calcium homeostasis, growth, differentiation, and biosynthesis pathways. Thus, dysfunction in this organelle represents a key factor in the activation of pathways of cell death, making it an attractive target for anti-trypanosomatid drugs [49–51]. By using JC-1 or Mitotracker labels, the results obtained demonstrate that **derivative 4,** in both concentrations used, affects the *L. amazonensis* mitochondrial function, which exhibited a pronounced reduction of its hydrogenionic membrane potential (ΔΨm). The disruption of ΔΨm can lead to leakage in the electron transport chain (ETC), and thus accelerate the generation of reactive oxygen species (ROS), such as superoxide anions, hydrogen peroxide, and hydroxyl radicals [52]. Thus, as a consequence of mitochondrial dysfunction triggering by depolarization of the mitochondrial membrane potential, **derivative 4** also induced a significant increase in the generation of ROS products. The disruption in mitochondrial functioning can rapidly culminate in a collapse in the bioenergetic metabolism of the parasite by decreasing the ATP synthesis, consequently causing cell death [53].

After observing the mitochondrial dysfunction triggered by the action of **derivative 4**, and considering its critical role for initiation of the cell death processes in the parasites, the activation of apoptosis-*like* was investigated. Associated with mitochondrial dysfunction, some biochemical hallmarks of this cell death pathway were also observed after treatment with **derivative 4**, such as: (i) the loss of asymmetry of

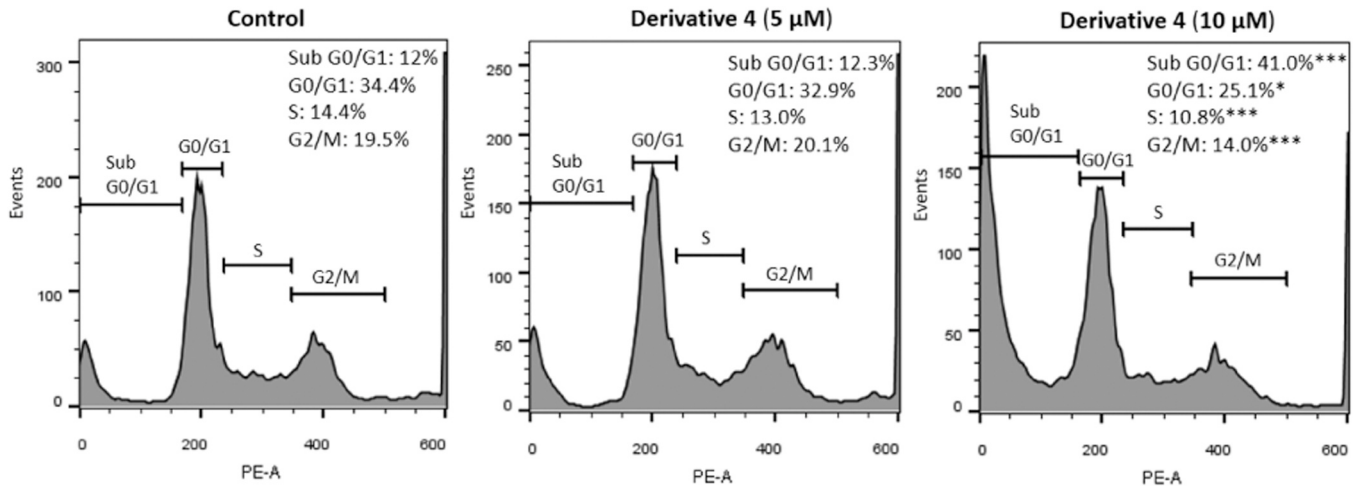

Fig. 6. Analysis of the cell cycle progression of *L. amazonensis*-promastigotes treated with derivative 4. Parasites (10^7 cells) were incubated without (non-treated control) or with **derivative 4** (5.0 or 10.0 µM) for 24 h. Afterward, cells were stained with propidium iodide (PI), and the analysis of DNA content was performed by flow cytometry. Data were expressed as the means of three independent experiments, which were performed in triplicate. (*), (**) and (***) represents statistically significant difference in relation to the non-treated control ($P < 0.1$, $P < 0.01$ and $P < 0.001$, respectively).

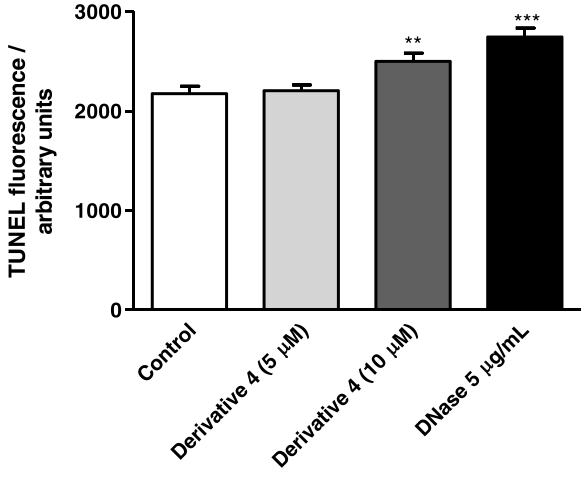

Fig. 7. Analysis of DNA fragmentation in derivative 4-treated *L. amazonensis* promastigotes. *Leishmania amazonensis* promastigotes were treated with **derivative 4** at 5 and 10 µM for 24 h and then a TUNEL assay was performed. The fluorescence intensity of TUNEL-positive parasites was evaluated using a fluorimetric microplate reader. DNase was used as a positive control. (**) and (***) represents statistically significant difference compared to the non-treated control ($P < 0.01$ and $P < 0.001$, respectively).

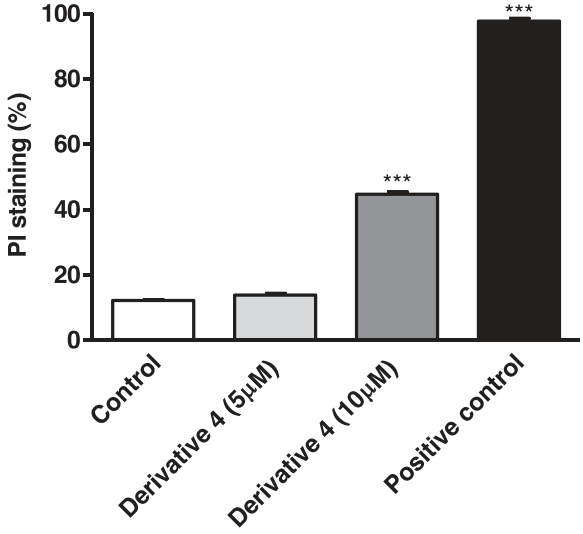

Fig. 8. Evaluation of the cell membrane integrity of *L. amazonensis* promastigotes treated with derivative 4. After treatment of parasites with **derivative 4** (5.0 or 10.0 µM) for 24 h, the permeabilization of plasma membrane was measured by incubation with propidium iodide (PI), and the fluorescence intensity was evaluated using a flow cytometry. (***) represents statistically significant difference in relation to the non-treated control ($P < 0.001$).

the plasma membrane with the externalization of anionic phospholipids to the cell surface, mainly PS; (ii) the nuclear DNA fragmentation, demonstrated by the TUNEL assay and the increase in the number of parasites with low DNA content (sub-G0/G1 phase) in cell cycle analysis, possibly triggered by excessive ROS production causing induction of DNA breaks; (iii) the deleterious effect of **derivative 4** in the cell division machinery of the parasite was more pronounced, affecting the cell cycle progression as evidenced by the decrease in G_0/G_1, S and G_2/M phases, interfering in the DNA replication with consequent cell cycle arrest and leading to the parasite death; and (iv) increase in neutral lipids detected by using the fluorescent indicator Nile Red. This latter alteration is suggestive of accumulation of lipid droplets, compartments containing high lipid content that regulate lipid metabolism, cell signaling and membrane trafficking [54]. The exacerbate formation of neutral lipids in this parasite has already been demonstrated after extensive oxidative stress and mitochondrial damage induced by drug treatment and is also closely associated with apoptosis-*like* [55,56].

These lipid structures have also been reported in *L. amazonensis* and *T. cruzi* treated with triazole derivatives and, particularly for azole compounds, this process could be related to the accumulation of lipid precursors resulting from the inhibition of ergosterol biosynthesis, causing changes in phospholipids and sterol content of the parasite membrane [57,58].

In addition, our results showed significant permeabilization of plasma membrane in the **derivative 4**-treated parasites, a typical feature of cell death by necrosis. This damage in the plasma membrane may have been caused by: (i) excess of ROS accumulation that can induce toxic effects to lipids and proteins; (ii) interference in the phospholipids and sterol content of the plasma membrane resulting from depletion of ergosterol biosynthesis, a pathway that has been widely described for the action of triazole derivatives in trypanosomatids and fungi [58–60]. Alterations in the composition of the plasma membrane can be lethal to parasites, causing formation of pores in the membrane

and alteration in pH control and transport of ions, metabolites and nutrients; which can lead to loss of cytoplasmic content, culminating in osmotic collapse of parasites and consequent cell death by necrosis-*like* [61].

In our work, by using flow cytometry, with the same doses and time of incubation (10.0 μM and 24 h, respectively), it was possible to discriminate subpopulations of treated parasites in early apoptosis-*like* (annexin V^+/PI^-; 17.3%), late apoptosis-*like* (annexin V^+/PI^+; 31.9%) and necrosis (annexin V^-/PI^+; 22.3%). By annexin V^+/PI^+ staining, it is plausible that the occurring necrotic process consists of secondary necrosis, since a similar phenotype has been observed in cell death processes induced by other antileishmanial molecules [62–64]. Moreover, strong mitochondrial deleterious effects and oxidative stress have been evidenced in secondary necrosis pathway after stimulus with different antileishmanial drugs, providing more evidence for the occurrence of this phenotype caused by **derivative 4** [64–67]. In the literature, it has been described that cells under the process of secondary necrosis present a remarkable and specific phenotype that accumulate apoptotic features, such as nuclear fragmentation associated to typical necrotic alterations, such as plasma membrane permeabilization [64,68–71]. Therefore, secondary necrosis has been reported as an essential process in the outcome of the complete apoptosis-*like*, being implicated as the endpoint in the mode of action of different classes of anti-trypanosomatid drugs [64,66,71–74]. Furthermore, parasites treated with the **compound 4** also showed annexin V^-/PI^+ staining, indicating that a subpopulation of the parasites presented signs of primary necrosis. As a limitation of our study, the investigations about the mode of antileishmanial action of **derivative 4** were not performed in a kinetics study at different time points after treatment, restricting knowledge about the sequence of the cellular events that resulted in cell death by necrosis. It is possible that the apoptosis and necrosis pathways are interconnected and further studies are required to better understand the triggers involved in parasite cell death.

Although not fully understood, the occurrence of more than one death process associated with a single drug (same or different concentrations) or drug associations is observed in trypanosomatids, as well as related to different *Leishmania* species. For example, Yangambin, a lignin, induces apoptosis in promastigotes of *L. amazonensis*, and promotes autophagy in *L. chagasi* [75]. Promastigotes of *L. donovani* treated with H_2O_2 doses above 4 mM exhibited a necrosis-*like* death, while apoptosis-*like* is observed in parasites treated at doses below 4 mM [76]. Two dibenzylideneacetones (A3K2A1 and A3K2A3), at the same dose, induced biochemical and morphological alterations in trypomastigotes and amastigotes of *Trypanosoma cruzi* associated with three pathways, apoptosis, autophagy and necrosis [67]. This research group has also reported that antileishmanial drugs in combination, like thiosemicarbazone and miltefosine, induce both autophagy and apoptosis [63]. Amioradone, an antiarrhythmic drug used for the symptomatic treatment of chronic Chagas' disease, showed inhibition of the growth of *L. amazonensis* and necrosis, apoptosis and/or autophagy were incriminated in the parasite death [67]. Additionally, in a recent review, Das and colleagues [71] discussed about the occurrence of multiple death processes simultaneously; and some authors pointed the permeabilization of the mitochondrial membranes as a crucial step in activation of apoptosis and necrosis pathways [77].

Together, this set of results leads to the overall hypothesis that **derivative 4** induces alterations in critical biochemical processes, which are essential for the correct functioning of organelles and macromolecules of the parasite, through interference in the bioenergetic system and plasma membrane permeabilization, with consequent activation of apoptosis-*like* and necrosis, ultimately culminating in cellular collapse.

In conclusion, the results suggest that **derivative 4**, a new quinoline triazole hybrid, is a promising lead compound for the treatment of leishmaniasis, which should be further explored through more detailed studies in murine models of *Leishmania* infection.

Acknowledgements

The authors would like to acknowledge the 'Programa de Pós-Graduacão em Ciências Biológicas (Universidade Federal de Juiz de Fora)' for allowing the use of the FACsCanto II flow cytometer multiuser equipment facility. This work received financial support from FAPEMIG, CAPES and CNPq. LMRA, ADS, EAFC and ESC receive grants from CNPq. NG receives grant from CAPES.

Conflicts of interest

The authors confirm that they have no conflicts of interest in relation to this work.

Appendix A. Supporting information

Supplementary data associated with this article can be found in the online version at doi:10.1016/j.biopha.2021.111857.

References

[1] J. Alvar, I.D. Vélez, C. Bern, M. Herrero, P. Desjeux, J. Cano, J. Jannin, M. den Boer, Leishmaniasis Control Team WHO, Leishmaniasis worldwide and global estimates of its incidence, PLoS One 7 (2012) 35671, https://doi.org/10.1371/journal.pone.0035671.
[2] World Health Organization Leishmaniasis, 2020 ⟨http://www.who.int/topics/leishmaniasis/en/⟩. (accessed 2 December 2020).
[3] S. Burza, S.L. Croft, M. Boelaert, Leishmaniasis, Lancet 392 (10151) (2018) 951–970, https://doi.org/10.1016/S0140-6736(18)31204-2.
[4] J.A.L. Lindoso, C.H.V. Moreira, M.A. Cunha, I.T. Queiroz, Visceral leishmaniasis and HIV coinfection: current perspectives, HIV AIDS (Auckl.) 10 (2018) 193–201, https://doi.org/10.2147/hiv.s143929.
[5] S.R.B. Uliana, C.T. Trinconi, A.C. Coelho, Chemotherapy of leishmaniasis: present challenges, Parasitology 145 (4) (2018) 464–480, https://doi.org/10.1017/s0031182016002523.
[6] S.S. Braga, Multi-target drugs active against leishmaniasis: a paradigm of drug repurposing, Eur. J. Med. Chem. 183 (2019), 111660, https://doi.org/10.1016/j.ejmech.2019.111660.
[7] Y.Q. Hu, C. Gao, S. Zhang, L. Xu, Z. Xu, L.S. Feng, X. Wu, F. Zhao, Quinoline hybrids and their antiplasmodial and antimalarial activities, Eur. J. Med. Chem. 139 (2017) 22–47, https://doi.org/10.1016/j.ejmech.2017.07.061.
[8] X.M. Chu, C. Wang, W. Liu, L.L. Liang, K.K. Gong, C.Y. Zhao, K.L. Sun, Quinoline and quinolone dimers and their biological activities: an overview, Eur. J. Med. Chem. 161 (2019) 101–117, https://doi.org/10.1016/j.ejmech.2018.10.035.
[9] N. Razzaghi-Asl, S. Sepehri, A. Ebadi, P. Karami, N. Nejatkhah, M. Johari-Ahar, Insights into the current status of privileged N-heterocycles as antileishmanial agents, Mol. Divers 24 (2) (2020) 525–569, https://doi.org/10.1007/s11030-019-09953-4.
[10] O. Afzal, S. Kumar, M.R. Haider, M.R. Ali, R. Kumar, M. Jaggi, S. Bawa, A review on anticancer potential of bioactive heterocycle quinoline, Eur. J. Med. Chem. 97 (2015) 871–910, https://doi.org/10.1016/j.ejmech.2014.07.044.
[11] M. Mishra, V.K. Mishra, V. Kashaw, A.K. Iyer, S.K. Kashaw, Comprehensive review on various strategies for antimalarial drug discovery, Eur. J. Med. Chem. 125 (2017) 1300–1320, https://doi.org/10.1016/j.ejmech.2016.11.025.
[12] N. Chokkar, S. Kalra, M. Chauhan, R. Kumar, A review on quinoline derived scaffolds as anti-HIV agents, Mini Rev. Med. Chem. 19 (6) (2019) 510–526, https://doi.org/10.2174/1389557518666181018163448.
[13] R.S. Keri, A.S. Patil, Quinoline: a promising antitubercular target, Biomed. Pharm. 68 (8) (2014) 1161–1175, https://doi.org/10.1016/j.biopha.2014.10.007.
[14] K. Bozorov, J. Zhao, H. Aisa, 1,2,3-Triazole-containing hybrids as leads in medicinal chemistry: a recent overview, Bioorg. Med. Chem. 27 (16) (2019) 3511–3531, https://dx.doi.org/10.1016%2Fj.bmc.2019.07.005.
[15] Z. Xu, S.J. Zhao, Y. Liu, 1,2,3-Triazole-containing hybrids as potential anticancer agents: current developments, action mechanisms and structure-activity relationships, Eur. J. Med. Chem. 183 (2019), 111700, https://doi.org/10.1016/j.ejmech.2019.111700.
[16] B. Zhang, Comprehensive review on the anti-bacterial activity of 1,2,3-triazole hybrids, Eur. J. Med. Chem. 168 (2019) 357–372, https://doi.org/10.1016/j.ejmech.2019.02.055.
[17] K.R. Begnini, W.R. Duarte, L.P. da Silva, J.H. Buss, B.S. Goldani, M. Fronza, N. V. Segatto, D. Alves, L. Savegnago, F.K. Seixas, T. Collares, Apoptosis induction by 7-chloroquinoline-1,2,3-triazoyl carboxamides in triple negative breast cancer cells, Biomed. Pharm. 91 (2017) 510–516, https://doi.org/10.1016/j.biopha.2017.04.098.
[18] P.H.F. Stroppa, L.M.R. Antinarelli, A.M.L. Carmo, J. Gameiro, E.S. Coimbra, A. D. da Silva, Effect of 1,2,3-triazole salts, non-classical bioisosteres of miltefosine, on *Leishmania amazonensis*, Bioorg. Med. Chem. 25 (2017) 3034–3045, https://doi.org/10.1016/j.bmc.2017.03.051.
[19] A. Upadhyay, P. Kushwaha, S. Gupta, R.P. Dodda, K. Ramalingam, R. Kant, N. Goyal, K.V. Sashidhara, Synthesis and evaluation of novel triazolyl quinoline

derivatives as potential antileishmanial agents, Eur. J. Med. Chem. 154 (2018) 172–181, https://doi.org/10.1016/j.ejmech.2018.05.014.
[20] R.R. Teixeira, P.A.R. Gazolla, A.M. da Silva, M.P.G. Borsodi, B.R. Bergmann, R. S. Ferreira, B.G. Vaz, G.A. Vasconcelos, W.P. Lima, Synthesis and leishmanicidal activity of eugenol derivatives bearing 1,2,3-triazole functionalities, Eur. J. Med. Chem. 146 (2018) 274–286, https://doi.org/10.1016/j.ejmech.2018.01.046.
[21] J.I. Manzano, J. Konstantinović, D. Scaccabarozzi, A. Perea, A. Pavić, L. Cavicchini, N. Basilico, F. Gamarro, B.A. Šolaja, 4-Aminoquinoline-based compounds as antileishmanial agents that inhibit the energy metabolism of Leishmania, Eur. J. Med. Chem. 180 (2019) 28–40, https://doi.org/10.1016/j.ejmech.2019.07.010.
[22] K. Balaraman, N.C. Vieira, F. Moussa, J. Vacus, S. Cojean, S. Pomel, C. Bories, B. Figadère, V. Kesavan, P.M. Loiseau, In vitro and in vivo antileishmanial properties of a 2-n-propylquinoline hydroxypropyl b-cyclodextrin formulation and pharmacokinetics via intravenous route, Biomed. Pharm. 76 (2015) 127–133, https://doi.org/10.1016/j.biopha.2015.10.028.
[23] A.M. Carmo, F.M. Silva, P.A. Machado, A.P. Fontes, F.R. Pavan, C.Q. Leite, S. R. Leite, E.S. Coimbra, A.D. Da Silva, Synthesis of 4-aminoquinoline analogues and their platinum(II) complexes as new antileishmanial and antitubercular agents, Biomed. Pharm. 65 (3) (2011) 204–209, https://doi.org/10.1016/j.biopha.2011.01.003.
[24] L.M. Antinarelli, R.M. Dias, I.O. Souza, W.P. Lima, J. Gameiro, A.D. da Silva, E. S. Coimbra, 4-Aminoquinoline derivatives as potential antileishmanial agents, Chem. Biol. Drug Des. 86 (4) (2015) 704–714, https://doi.org/10.1111/cbdd.12540.
[25] R.S. Meinel, A.D.C. Almeida, P.H.F. Stroppa, N. Glanzmann, E.S. Coimbra, A.D. da Silva, Novel functionalized 1,2,3-triazole derivatives exhibit antileishmanial activity, increase in total and mitochondrial-ROS and depolarization of mitochondrial membrane potential of *Leishmania amazonensis*, Chem. Biol. Inter. 315 (2020), 108850, https://doi.org/10.1016/j.cbi.2019.108850.
[26] L.M. Antinarelli, A.M. Carmo, F.R. Pavan, C.Q. Leite, A.D. Da Silva, E.S. Coimbra, D.B. Salunke, Increase of leishmanicidal and tubercular activities using steroids linked to aminoquinoline, Org. Med. Chem. Lett. 2 (16) (2012) 1–8, https://doi.org/10.1186/2191-2858-2-16.
[27] M.P. Rodrigues, D.C. Tomaz, L.A. Souza, T.S. Onofre, W.A. Menezes, J. Almeida-Silva, A.M. Suarez-Fontes, M.R. Almeida, A.M. Silva, G.C. Bressan, M.A. Vannier-Santos, J.L. Fietto, R.R. Teixeira, Synthesis of cinnamic acid derivatives and leishmanicidal activity against *Leishmania braziliensis*, Eur. J. Med Chem. 183 (2019), 111688, https://doi.org/10.1016/j.ejmech.2019.111688.
[28] J.L. Luco, A.I. Recio-Balsells, D.G. Ghiano, A. Bortolotti, J.M. Belardinelli, N. Liu, P. Hoffmann, C. Lherbet, P.J. Tonge, B. Tekwani, H.R. Morbidoni, G.R. Labadie, Exploring the chemical space of 1,2,3-triazolyl triclosan analogs for discovery of new antileishmanial chemotherapeutic agentes, RSC Med. Chem. 12 (2021) 120–128, https://doi.org/10.1039/D0MD00291G.
[29] T.T. Guimarães, M.C. Pinto, J.S. Lanza, M.N. Melo, R.L. Monte-Neto, I.M. Melo, E. B. Diogo, V.F. Ferreira, C.A. Camara, W.O. Valença, R.N. Oliveira, F. Frézard, E. M. Silva Júnior, Potent naphthoquinones against antimony-sensitive and -resistant *Leishmania* parasites: synthesis of novel a- and nor-a-lapachonebased 1,2,3-triazoles by copper-catalyzed azideealkyne cycloaddition, Eur. J. Med. Chem. 63 (2013) 523–530, https://doi.org/10.1016/j.ejmech.2013.02.038.
[30] N.B. De Souza, A.M. Carmo, A.D. da Silva, T.C. França, A.U. Krettli, Antiplasmodial activity of chloroquine analogs against chloroquine-resistant parasites, docking studies and mechanisms of drug action, Malar. J. 13 (2014) 469, https://doi.org/10.1186/2191-2858-2-16.
[31] J.M. Ren, J.T. Wiltshire, A. Blencowe, G.G. Qiao, Synthesis of a star polymer library with a diverse range of highly functionalized macromolecular architectures, Macromolecules 44 (2011) 3189–3202, https://doi.org/10.1021/ma200283c.
[32] E.S. Coimbra, L.M. Antinarelli, A.D. da Silva, M.L. Bispo, C.R. Kaiser, M.V. de Souza, 7-Chloro-4-quinolinyl hydrazones: a promising and potent class of antileishmanial compounds, Chem. Biol. Drug Des. 81 (5) (2013) 658–665, https://doi.org/10.1111/cbdd.12112.
[33] E.S. Coimbra, M.V.N. de Souza, M.S. Terror, A.C. Pinheiro, J.T. Granato, Synthesis, biological activity, and mechanism of action of new 2-pyrimidinyl hydrazone and N-acylhydrazone derivatives, a potent and new classes of antileishmanial agents, Eur. J. Med. Chem. 184 (2019), 111742, https://doi.org/10.1016/j.ejmech.2019.111742.
[34] C. Yang, L. Jiang, H. Zhang, L.A. Shimoda, R.J. DeBerardinis, G.L. Semenza, Chapter twenty-two - analysis of hypoxia-induced metabolic reprogramming, Methods Enzymol. 542 (2014) 425–455, https://doi.org/10.1016/B978-0-12-416618-9.00022-4.
[35] S. Saini, K. Bharati, C. Shaha, C.K. Mukhopadhyay, Zinc depletion promotes apoptosis-like death in drug-sensitive and antimony-resistance *Leishmania donovani*, Sci. Rep. 7 (2017) 10488, https://doi.org/10.1038/s41598-017-10041-6.
[36] L.M.R. Antinarelli, I. de Oliveira Souza, P.V. Zabala Capriles, J. Gameiro, E. A. Britta, C.V. Nakamura, W.P. Lima, A.D. da Silva, E.S. Coimbra, Antileishmanial activity of a 4-hydrazinoquinoline derivative: induction of autophagy and apoptosis-related processes and effectiveness in experimental cutaneous leishmaniasis, Exp. Parasitol. 195 (2018) 78–86, https://doi.org/10.1016/j.exppara.2018.10.007.
[37] L.M.R. Antinarelli, R.S. Meinel, E.A.F. Coelho, A.D. da Silva, E.S. Coimbra, Resveratrol analogues present effective antileishmanial activity against promastigotes and amastigotes from distinct *Leishmania* species by multitarget action in the parasites, J. Pharm. Pharmacol. 71 (12) (2019) 1854–1863, https://doi.org/10.1111/jphp.13177.
[38] L. Thakur, K.K. Singh, V. Shanker, A. Negi, A. Jain, G. Matlashewski, M. Jain, Atypical leishmaniasis: a global perspective with emphasis on the Indian subcontinent, PLoS Negl. Trop. Dis. 12 (9) (2018), 0006659, https://doi.org/10.1371/journal.pntd.0006659.
[39] N. Boechat, M.L. Ferreira, L.C. Pinheiro, A.M. Jesus, M.M. Leite, C.C. Júnior, A. C. Aguiar, I.M. Andrade, A.U. Krettli, New compounds hybrids 1H-1,2,3-triazole-quinoline against *Plasmodium falciparum*, Chem. Biol. Drug Des. 84 (2014) 325–332, https://doi.org/10.1111/cbdd.12321.
[40] A.R. Hamann, C. Kock, P.J. Smith, W.A. Otterlo, M.A. Blackie, Synthesis of novel triazole-linked mefloquine derivatives: Biological evaluation against *Plasmodium falciparum*, Bioorg. Med. Chem. Lett. 24 (2014) 5466–5469, https://doi.org/10.1016/j.bmcl.2014.10.015.
[41] A. Singh, J. Gut, P.J. Rosenthal, V. Kumar, 4-Aminoquinoline-ferrocenyl-chalcone conjugates: synthesis and anti-plasmodial evaluation, Eur. J. Med. Chem. 125 (2017) 269–277, https://doi.org/10.1016/j.ejmech.2016.09.044.
[42] D.R. Melis, C.B. Barnett, L. Wiesner, E. Nordlander, G.S. Smith, Quinoline-triazole half-sandwich iridium(III) complexes: synthesis, antiplasmodial activity and preliminary transfer hydrogenation studies, Dalton Trans. 49 (2020) 11543–11555, https://doi.org/10.1039/D0DT01935F.
[43] K.R. Begnini, W.R. Duarte, L.P. Silva, J.H. Buss, B.S. Goldani, M. Fronza, N. V. Segatto, D. Alves, L. Savegnago, F.K. Seixas, T. Collares, Apoptosis induction by 7-chloroquinoline-1,2,3-triazoyl carboxamides in triple negative breast cancer cells, Biomed. Pharm. 91 (2017) 510–516, https://doi.org/10.1016/j.biopha.2017.04.098.
[44] K.K. Kumar, S.P. Seenivasan, V. Kumar, T.M. Das, Synthesis of quinoline coupled [1,2,3]-triazoles as a promising class of anti-tuberculosis agentes, Carbohydr. Res. 346 (2011) 2084–2090, https://doi.org/10.1016/j.carres.2011.06.028.
[45] V. Sumangala, B. Poojary, N. Chidananda, J. Fernandes, N.S. Kumari, Synthesis and antimicrobial activity of 1,2,3-triazoles containing quinoline moiety, Arch. Pharm. Res. 33 (12) (2010) 1911–1918, https://doi.org/10.1007/s12272-010-1204-3.
[46] P.P. Thakare, A.D. Shinde, P.C. Abhijit, N.V. Nyayanit, V.D. Bobade, P.C. Mhaske, Synthesis and biological evaluation of new 1,2,3-triazolylpyrazolyl-quinoline derivatives as potential antimicrobial agents, ChemistrySelect 5 (2020) 4722–4727, https://doi.org/10.1002/slct.201904455.
[47] M. Irfan, S. Alam, N. Manzoor, M. Abid, Effect of quinoline based 1,2,3-triazole and its structural analogues on growth and virulence attributes of Candida albicans, Plos One 12 (4) (2017), e0175710, https://doi.org/10.1371/journal.pone.0175710.
[48] S.P. Mantoani, T.P. Chierrito, A.F. Vilela, C.L. Cardoso, A. Martínez, I. Carvalho, Novel triazole-quinoline derivatives as selective dual binding site acetylcholinesterase inhibitors, Molecules 21 (2016) 193, https://doi.org/10.3390/molecules21020193.
[49] L. Monzote, L. Gille, Mitochondria as a promising antiparasitic target, Curr. Clin. Pharm. 5 (1) (2010) 55–60, https://doi.org/10.2174/157488410790410605.
[50] D. Smirlis, M. Duszenko, A.J. Ruiz, E. Scoulica, P. Bastien, N. Fasel, K. Soteriadou, Targeting essential pathways in trypanosomatids gives insights into protozoan mechanisms of cell death, Parasit. Vectors 3 (2010) 107, https://doi.org/10.1186/1756-3305-3-107.
[51] M. Amaral, F.S. de Sousa, T.A.C. Silva, A.J.G. Junior, N.N. Taniwaki, D.M. Johns, J. H.G. Lago, E.A. Anderson, A.G. Tempone, A semi-synthetic neolignan derivative from dihydrodieugenol B selectively affects the bioenergetic system of *Leishmania infantum* and inhibits cell division, Sci. Rep. 9 (1) (2019) 6114, https://doi.org/10.1038/s41598-019-42273-z.
[52] C. Pal, U. Bandyopadhyay, Redox-active antiparasitic drugs, Antioxid. Redox Signal 17 (4) (2012) 555–582, https://doi.org/10.1089/ars.2011.4436.
[53] N. Miranda, H. Volpato, J.H. da Silva Rodrigues, W. Caetano, T. Ueda-Nakamura, S. de Oliveira Silva, C.V. Nakamura, The photodynamic action of pheophorbide a induces cell death through oxidative stress *in Leishmania amazonensis*, J. Photochem. Photobiol. B. 174 (2017) 342–354, https://doi.org/10.1016/j.jphotobiol.2017.08.016.
[54] E. Jarc, T. Petan, Lipid droplets and the management of cellular stress, Yale J. Biol. Med. 92 (3) (2019) 435–452, 20.
[55] J. Boren, K.M. Brindle, Apoptosis-induced mitochondrial dysfunction causes cytoplasmic lipid droplet formation, Cell Death Differ. 19 (9) (2012) 1561–1570, https://doi.org/10.1038/cdd.2012.34.
[56] S. Lee, J. Zhang, A.M. Choi, H.P. Kim, Mitochondrial dysfunction induces formation of lipid droplets as a generalized response to stress, Oxid. Med. Cell Longev. 2013 (2013), 327167, https://doi.org/10.1155/2013/327167.
[57] J.C. Fernandes Rodrigues, J.L. Concepcion, C. Rodrigues, A. Caldera, J.A. Urbina, W. de Souza, In vitro activities of ER-119884 and E5700, two potent squalene synthase inhibitors, against *Leishmania amazonensis*: antiproliferative, biochemical, and ultrastructural effects, Antimicrob. Agents Chemother. 52 (11) (2008) 4098–4114, https://dx.doi.org/10.1128%2FAAC.01616-07.
[58] S.T. De Macedo-Silva, G. Visbal, J.A. Urbina, W. de Souza, J.C. Rodrigues, Potent in vitro antiproliferative synergism of combinations of ergosterol biosynthesis inhibitors against *Leishmania amazonensis*, Antimicrob. Agents Chemother. 59 (10) (2015) 6402–6418, https://dx.doi.org/10.1128%2FAAC.01150-15.
[59] S.T. De Macedo-Silva, J.A. Urbina, W. de Souza, J.C. Rodrigues, In vitro activity of the antifungal azoles itraconazole and posaconazole against *Leishmania amazonensis*, PLoS One 8 (12) (2013) 83247, https://doi.org/10.1371/journal.pone.0083247.
[60] K. Figarella, S. Marsiccobetre, I. Arocha, W. Colina, M. Hasegawa, M. Rodriguez, A. Rodriguez-Acosta, M. Duszenko, G. Benaim, N.L. Uzcategui, Ergosterone-coupled Triazol molecules trigger mitochondrial dysfunction, oxidative stress, and acidocalcisomal Ca2+ release in *Leishmania mexicana* promastigotes, Micro Cell 3 (1) (2015) 14–28, https://doi.org/10.15698/mic2016.01.471.
[61] E. Umehara, T.A. Costa Silva, V.M. Mendes, R.C. Guadagnin, P. Sartorelli, A. G. Tempone, J.H.G. Lago, Differential lethal action of C17:2 and C17:0 anacardic

acid derivatives in *Trypanosoma cruzi* - a mechanistic study, Bioorg. Chem. 102 (2020), 104068, https://doi.org/10.1016/j.bioorg.2020.104068.
[62] V. Gómez-Pérez, J.I. Manzano, R. Garciá-Hernández, S. Castanys, J.M. Rosa, F. Gamarro, 4-Amino bis-pyridinium derivatives as novel antileishmanial agents, Antimicrob. Agents Chemother. 58 (2014) 4103–4112, https://doi.org/10.1128/AAC.02481-13.
[63] D.B. Scariot, E.A. Britta, A.L. Moreira, H. Falzirolli, C.C. Silva, T. Ueda-Nakamura, B.P. Dias-Filho, C.V. Nakamura, Induction of early autophagic process on *Leishmania amazonensis* by synergistic effect of miltefosine and innovative semi-synthetic Thiosemicarbazone, Front Microbiol 8 (2017) 255, https://doi.org/10.3389/fmicb.2017.00255.
[64] D.B. Scariot, H. Volpato, N.S. Fernandes, E.F.P. Soares, T. Ueda-Nakamura, B. P. Dias-Filho, Z.U. Din, E. Rodrigues-Filho, A.F. Rubira, O. Borges, M.D.C. Sousa, C. V. Nakamura, Activity and cell-death pathway in *Leishmania infantum* induced by sugiol: vectorization using yeast cell wall particles obtained from Saccharomyces cerevisiae, Front Cell Infect. Microbiol 9 (2019) 208, https://doi.org/10.3389/fcimb.2019.00208.
[65] J.D. Inacio, M.M. Canto-Cavalheiro, R.F. Menna-Barreto, E.E. Almeida-Amaral, Mitochondrial damage contribute to epigallocatechin-3-gallate induced death *in Leishmania amazonensis*, Exp. Parasitol. 132 (2) (2012) 151–155, https://doi.org/10.1016/j.exppara.2012.06.008.
[66] L. Cuevas, M.C. Moreno-Bondi, J.M. Alunda, Allicin induces calcium and mitochondrial dysregulation causing necrotic death in *Leishmania*, 3, PLoS Negl. Trop. Dis. 10 (10) (2016), 0004525, https://doi.org/10.1371/journal.pntd.0004525.
[67] S.T. de Macedo-Silva, T.L. de Oliveira Silva, J.A. Urbina, W. de Souza, J. C. Rodrigues, Antiproliferative, ultrastructural, and physiological effects of amiodarone on promastigote and amastigote forms of *Leishmania amazonensis*, Mol. Biol. Int 2011 (2011), 876021, https://doi.org/10.4061/2011/876021.
[68] N. Sen, B.B. Das, A. Ganguly, T. Mukherjee, S. Bandyopadhyay, H.K. Majumder, Camptothecin-induced imbalance in intracellular cation homeostasis regulates programmed cell death in unicellular hemoflagellate *Leishmania donovani*, J. Biol. Chem. 279 (2004) 52366–52375, https://doi.org/10.1074/jbc.M406705200.
[69] S.K. Ardestani, F. Poorrajab, S. Razmi, A. Foroumadi, S. Ajdary, B. Gharegozlou, M. Behrouzi-Fardmoghadam, A. Shafiee, Cell death features induced in *Leishmania major* by 1,3,4-thiadiazole derivatives, Exp. Parasitol. 132 (2) (2012) 116–122, https://doi.org/10.1016/j.exppara.2012.06.002.
[70] M.T. Silva, Secondary necrosis: the natural outcome of the complete apoptotic program, FEBS Lett. 584 (22) (2010) 4491–4499, https://doi.org/10.1016/j.febslet.2010.10.046.
[71] P. Das, S. Saha, S. BoseDasgupta, The ultimate fate determinants of drug induced cell-death mechanisms in Trypanosomatids, Int. J. Parasitol. Drugs Drug Resist 15 (2021) 81–91, https://dx.doi.org/10.1016%2Fj.ijpddr.2021.01.003.
[72] D. Lazarin-Bidóia, V.C. Desoti, S.C. Martins, F.M. Ribeiro, Z. Ud Din, E. Rodrigues-Filho, T. Ueda-Nakamura, C.V. Nakamura, S. de Oliveira Silva, Dibenzylideneacetones are potent trypanocidal compounds that affect the *Trypanosoma cruzi* redox system, Antimicrob. Agents Chemother. 60 (2) (2015) 890–903, https://doi.org/10.1128/AAC.01360-15.
[73] R.F. Menna-Barreto, Cell death pathways in pathogenic trypanosomatids: lessons of (over)kill, Cell Death Dis. 10 (2019) 93, https://doi.org/10.1038/s41419-019-1370-2.
[74] P.L. Sousa, Souza RODS, L.D. Tessarolo, R.R.P.P.B. de Menezes, T.L. Sampaio, J. A. Canuto, A.M.C. Martins, Betulinic acid induces cell death by necrosis in *Trypanosoma cruzi*, Acta Trop. 174 (2017) 72–75, https://doi.org/10.1016/j.actatropica.2017.07.003.
[75] R.L. Monte Neto, L.M. Sousa, C.S. Dias, J.M. Filho, M.R. Oliveira, R.C. Figueiredo, Morphological and physiological changes in *Leishmania* promastigotes induced by yangambin, a lignan obtained from Ocotea duckei, Exp. Parasitol. 127 (1) (2011) 215–221, https://doi.org/10.1016/j.exppara.2010.07.020.
[76] M. Das, S.B. Mukherjee, C. Shaha, Hydrogen peroxide induces apoptosis-like death in *Leishmania donovani* promastigotes, J. Cell Sci. 114 (13) (2001) 2461–2469.
[77] K.W. Kinnally, P.M. Peixoto, S. Ryu, L.M. Dejean, Is mPTP the gatekeeper for necrosis, apoptosis, or both? Biochim. Biophys. Acta 1813 (4) (2011) 612–622, https://doi.org/10.1016/j.bbamcr.2010.09.013.